Published in final edited form as:
Nat Neurosci. ; 15(1): 81–89. doi:10.1038/nn.2995.

Differential control of presynaptic efficacy by postsynaptic N-cadherin and β-catenin

Nathalia Vitureira[1], **Mathieu Letellier**[1], **Ian J. White**[1], and **Yukiko Goda**[1,2]

[1]MRC Laboratory for Molecular Cell Biology and Cell Biology Unit University College London, Gower Street, London WC1E 6BT, UK

[2]RIKEN Brain Science Institute, Wako, Saitama 351-0198, Japan

Abstract

N-cadherin is a homophilic adhesion protein that remains expressed at mature excitatory synapses beyond its developmental role in synapse formation. We have investigated the transsynaptic activity of N-cadherin in regulating synapse function in rodent cultured hippocampal neurons using optical methods and electrophysiology. Interfering with N-cadherin in postsynaptic neurons reduces basal release probability (p_r) at inputs to the neuron, and this transsynaptic impairment of release accompanies impaired vesicle endocytosis. Moreover, the loss of GluA2, which decreases p_r by itself, occludes the effect of interfering with postsynaptic N-cadherin. The loss of postsynaptic N-cadherin activity, however, does not affect the compensatory upregulation of p_r induced by activity silencing, while postsynaptic β-catenin deletion blocks this presynaptic homeostatic adaptation. Our findings suggest that postsynaptic N-cadherin plays a role in linking basal pre- and postsynaptic strengths to control the level of p_r offset while the gain adjustment of p_r requires a distinct transsynaptic pathway involving β-catenin.

INTRODUCTION

The formation and morphogenesis of nascent synaptic contacts are assisted by adhesion proteins, including cadherins that mediate Ca^{2+}-dependent homophilic intercellular interactions. Recent studies highlight roles for N-cadherin, the most widely expressed classical cadherin family member in neurons, in regulating dendritic spine morphology and synaptic efficacy beyond its established function in shaping developing synaptic networks. Interfering with N-cadherin-dependent adhesion not only produces fewer synapses[1] but increases dendritic spines with immature morphology[1-4], reduces synaptic vesicle (SV) cluster size and turnover[1,3,4], and impairs synaptic plasticity[5,6]. Furthermore, loss of N-cadherin expression also accompanies spine shrinkage and defects in long-term potentiation[7-9] and short-term synaptic plasticity[10,11].

Neurotransmitter release probability (p_r) is a key presynaptic determinant of synaptic efficacy, and it is dynamically altered during synaptic plasticity. Moreover, p_r is highly heterogeneous amongst different synapses, even for those formed onto single neurons[12-14]. Over the past decades, our understanding of the mechanisms of p_r regulation has significantly advanced, particularly with respect to the contribution of intracellular Ca^{2+} dynamics and Ca^{2+}-binding proteins[15,16]. However, we know very little about how basal p_r

Correspondence should be addressed to Y.G. (goda@brain.riken.jp)..

AUTHOR CONTRIBUTIONS N.V. performed all of the experimental work. M.L. contributed electrophysiology experiments and discussion, and I.W. performed electron microscopy work. N.V. and Y.G. designed the project and wrote the manuscript.

The authors declare no competing financial interests.

Europe PMC Funders Author Manuscripts

is set at individual synapses, and how p_r is homeostatically adjusted according to changes in network activity. Recent studies have suggested that p_r is set retrogradely in a manner compensatory to postsynaptic activity[17,18] and that such regulation is implemented locally at the level of dendritic branches[17]. Although molecular mechanisms of the retrograde control of p_r remain to be delineated, both diffusible molecules[19,20] and synapse adhesion proteins[21,22] have been implicated in this process.

Here, we have explored whether N-cadherins via its homophilic interactions, could directionally control synaptic strength and contribute to the retrograde regulation of p_r. We have previously shown that postsynaptic N-cadherin/β-catenin complex modulates synaptic AMPA receptor (AMPAR) abundance under basal conditions in a cell autonomous manner (in '*cis*')[5]. Furthermore, loss of β-catenin in postsynaptic neurons prevents homeostatic synaptic scaling of AMPARs induced by chronic changes in network activity. Here we find that interfering with N-cadherin activity selectively in postsynaptic neurons is sufficient to impair presynaptic strength in '*trans*', an effect which is occluded by the loss of GluA2. In contrast, the ability of synapses to homeostatically adapt p_r remains unaffected. Surprisingly, postsynaptic N-cadherin and β-catenin are differentially required for regulating presynaptic release in *trans*. Unlike N-cadherin, loss of postsynaptic β-catenin does not affect p_r but prevents homeostatic up-regulation of p_r induced by activity silencing. Our findings reveal two molecularly dissociable components of basal presynaptic strength regulation: one for setting the level of basal presynaptic strength and the other for adjusting the gain.

RESULTS

Postsynaptic N-cadherin affects presynaptic organization

To examine how postsynaptic N-cadherin regulated presynaptic organization and function transsynaptically, we interfered with N-cadherin activity in isolated neurons and studied the properties of presynaptic inputs formed onto such neurons. We first compared the effects of overexpressing C-terminally GFP-tagged wild type N-cadherin (WT-NCad), a dominant negative N-cadherin lacking the extracellular cadherin repeats required for effective intercellular adhesion (DN-NCad)[5], and a control GFP vector. Neurons were transfected at 10 days *in vitro* (DIV) following the initial wave of synaptogenesis. The low transfection efficiency (<10 neurons per coverslip) ensured that the majority of presynaptic inputs onto a transfected neuron originated from non-transfected control neurons (Fig. 1a,b). Consistent with a reported role for N-cadherins in synapse formation and maintenance[1], DN-NCad neurons received ~40% fewer synapses relative to controls, whereas WT-NCad had synapse density comparable to control neurons (data not shown). To assess whether postsynaptic N-cadherin affected the presynaptic organization transsynaptically, we determined the levels of synaptophysin, an abundant SV membrane protein, and bassoon, an active zone component, by immunofluorescence labeling (Fig. 1c,d; Suppl Fig. 1). Compared to synapses on control non-transfected neurons, synapses remaining on DN-NCad neurons showed decreased levels of synaptophysin and bassoon (fold respectively: DN-NCad, 0.85 ± 0.03 and 0.79 ± 0.06; WT-NCad, 1.05 ± 0.05 and 1.03 ± 0.07; GFP, 1.11 ± 0.05 and 0.98 ± 0.03), suggesting reduced SV number and active zone size upon transsynaptically impairing N-cadherin activity. We also determined the cell autonomous effect of DN-NCad on postsynaptic receptors in *cis*. Live labeling for surface GluA2 AMPAR subunit also revealed a specific reduction in synaptic GluA2 signal (apposed to synapsin I) in DN-NCad (0.78 ± 0.06; $P<0.01$) but not in WT-NCad neurons (1.03 ± 0.06; $P>0.2$) relative to controls (0.98 ± 0.03) (Fig. 1f), consistent with our previous observations on quantal amplitudes[5]. The level of total synaptic AMPAR, however, was not different for neurons expressing WT-NCad (0.98 ± 0.06; $P>0.2$), DN-NCad (1.14 ± 0.06; $P>0.2$), or control GFP (1.02 ± 0.08; $P>0.2$)

compared to untransfected cells on the same coverlip (Fig. 1e), suggesting that DN-NCad specifically altered the surface to intracellular distribution of AMPARs.

We next investigated the ultrastructural organization of presynaptic boutons on neurons transfected with the N-cadherin constructs by correlative light and serial electron microscopy (Fig. 2). Synapses had a normal appearance irrespective of whether they contacted the dendrites of WT-NCad, DN-NCad or control GFP neurons. However, quantification revealed a significant decrease in total SV number at boutons on DN-NCad neurons compared to control or WT-NCad neurons [DN-NCad, 132 ± 9 ($P<0.001$); WT-NCad, 237 ± 14; GFP, 245 ± 12]. Furthermore, the number of vesicles docked at the active zone was also reduced in presynaptic boutons on DN-NCad neurons relative to control GFP or WT-NCad neurons [DN-NCad, 3.0 ± 0.4 ($P<0.001$); WT-NCad, 6.0 ± 0.4; GFP, 7.0 ± 0.6]. These observations are consistent with results from immunofluorescence analysis for synaptophysin and bassoon, whose levels are decreased specifically in DN-NCad expressing neurons. Thus, postsynaptic expression of DN-NCad is sufficient to transsynaptically compromise the presynaptic organization. Notably, postsynaptic overexpression of WT-NCad has no effects on the presynaptic organization. This could be due to the limited availability of the NCad interacting proteins that are involved in the presynaptic regulation, such that excess postsynaptic NCad on its own is ineffective.

N-cadherin affects presynaptic efficacy in trans

To determine whether the presynaptic morphological changes induced by the postsynaptic DN-NCad were associated with functional changes, we monitored SV dynamics using the styryl dye FM4-64 or an antibody against the luminal domain of synaptotagmin I. Field stimulation [900 action potentials (APs) at 10 Hz] was applied to neurons in the presence of FM4-64 or the synaptotagmin antibody to label the total recycling pool of SVs (Fig. 3). The recycling pool size was significantly smaller in boutons on DN-NCad neurons but not on WT-NCad neurons relative to control neurons [in arbitrary units, FM dye: DN-NCad 411 ± 45 ($P<0.001$), WT-NCad 575 ± 29, GFP 629 ± 38; synaptotagmin: DN-NCad 124 ± 5 ($P<0.001$), WT-NCad 150 ± 7, GFP 159 ± 8]. To test whether this reduced recycling pool size accompanied a decrease in release probability, we performed optical quantal analysis to estimate p_r at individual synapses[13,23,24] (Fig. 4a,b). Boutons formed onto DN-NCad neurons showed a 42% reduction in p_r whereas no change was observed at WT-NCad neurons compared to GFP or non-transfected controls [DN-NCad 0.20 ± 0.01 ($P<0.001$), WT-NCad 0.33 ± 0.02, GFP 0.35 ± 0.03, untransfected 0.34 ± 0.03].

Intercellular adhesion mediated by classical cadherins is highly dependent on extracellular calcium[25]. We therefore wondered if the transsynaptic decrease in p_r caused by the postsynaptic expression of DN-NCad could be linked to the loss of Ca^{2+}-sensitivity of neurotransmitter release, for example, by affecting the organization or activity of Ca^{2+} channels. However, raising the extracellular Ca^{2+} from 2 to 5 mM increased p_r at synapses on DN-NCad neurons by ~50% (0.18 ± 0.02 to 0.28 ± 0.02), an extent comparable to the p_r increase observed at control GFP neurons under the same conditions (0.27 ± 0.01 to 0.41 ± 0.02)(Fig. 4c). Thus, despite the reduced p_r, synapses on DN-NCad neurons retain the capacity to respond to changes in extracellular Ca^{2+}. Since DN-NCad acts as a dominant negative for all classical cadherins, we confirmed the specificity for postsynaptic N-cadherin in regulating p_r using a short hairpin RNA (shRNA) to knock down endogenous N-cadherin in postsynaptic neurons. Presynaptic boutons on neurons expressing the shRNA, whose potency in reducing N-cadherin levels in hippocampal neurons had been previously confirmed[8], showed reduced p_r (0.15 ± 0.02%) relative to boutons on scrambled shRNA neurons (0.23 ± 0.01; $P<0.01$)(Suppl Fig. 2), and the extent decrease of p_r was comparable to that observed for DN-NCad expressing neurons (Fig. 4b). Therefore, loss of postsynaptic N-cadherin activity is sufficient to compromise neurotransmitter release in *trans*.

We also confirmed the specificity for postsynaptic N-cadherin impairment on presynaptic organization in *trans* and AMPAR levels in *cis* using the shRNA (Suppl Fig. 2). Bassoon, synaptophysin and surface GluA2 immunofluorescence intensity at synapses received by shRNA expressing neurons were significantly reduced compared to control scrambled shRNA neurons [fold relative to non-transfected neurons, bassoon: NC shRNA 0.64 ± 0.06, scramble 0.98 ± 0.04; synaptophysin: NC shRNA 0.70 ± 0.04, scramble 1.0 ± 0.07; surface GluA2: NC shRNA 0.67 ± 0.05, scramble 1.02 ± 0.07; (P<0.001)], similarly to the reduction we observed for the DN-NCad overexpression.

The major intracellular binding partner of N-cadherin is β-catenin, which, together with α-catenin, links cadherins to the F-actin cytoskeleton. To test whether β-catenin played a role in the transsynaptic modulation of presynaptic function by N-cadherin, we first examined if impairing N-cadherin activity altered the localization of β-catenin. The pattern of synaptic distribution of endogenous β-catenin was not appreciably changed in DN-NCad neurons compared to WT-NCad or control GFP neurons (Suppl Fig. 3). We next tested if the ability of postsynaptic N-cadherin to regulate presynaptic release required its interaction with β-catenin by overexpressing a mutant N-cadherin lacking the β-catenin binding region in its C-terminal domain (NC-ΔC)[5]. Synapses formed onto NC-ΔC neurons showed no differences in p_r compared to control neurons (NC-ΔC 0.28 ± 0.03, GFP 0.33 ± 0.02, P>0.2)(Suppl Fig. 2), suggesting that postsynaptic N-cadherin modulates presynaptic release in a β-catenin-independent manner. To further clarify whether β-catenin could regulate p_r in *trans*, we used cultures from β-catenin floxed mice[26] and knocked down endogenous β-catenin by expressing Cre in sparse number of neurons, and determined the consequence on presynaptic organization and function as described above. Neurons transfected with Cre-IRES-GFP at DIV10 showed a loss of β-catenin immunofluorescence labeling by DIV14 (Suppl Fig. 4a)[5]. In contrast to impairing postsynaptic N-cadherin activity, postsynaptic loss of β-catenin produced no changes in synaptophysin and bassoon levels compared to control IRES-GFP or non-transfected neurons (relative to non-transfected neurons, synaptophysin: Cre-IRES-GFP 0.96 ± 0.02, IRES-GFP 1.00 ± 0.03, P>0.2; bassoon: Cre-IRES-GFP 0.97 ± 0.06, IRES-GFP 0.99 ± 0.04, P>0.2)(Suppl Fig. 4c,d). Likewise, optical quantal analysis revealed no significant changes in p_r in boutons on β-catenin ablated neurons (0.28 ± 0.02) compared to boutons on control IRES-GFP neurons (0.25 ± 0.02, P>0.2)(Suppl Fig. 2). Altogether, these results suggest that the transsynaptic regulation of basal presynaptic strength does not require postsynaptic β-catenin. We also determined the effect of β-catenin loss on the level of postsynaptic AMPARs in *cis*. Synaptic GluA2 was reduced in β-catenin ablated neurons (0.92 ± 0.03 fold) compared to control IRES-GFP neurons (1.10 ± 0.04 fold; P<0.05)(Suppl Fig. 4e), consistent with our previous finding of a role for β-catenin in regulating synaptic AMPAR currents in *cis*[5].

To confirm our finding of transsynaptic regulation of neurotransmitter release by postsynaptic N-cadherin in an independent assay, we performed whole-cell patch clamp recordings from connected cell pairs in which the postsynaptic neuron overexpressed WT-NCad, DN-NCad or control GFP, or shRNA for N-cadherin or control scrambled shRNA. Short-term depression is a form of plasticity in which the extent depression of postsynaptic responses to successive stimulation correlates with the initial p_r, with synapses having higher p_r producing larger depression and those with lower p_r showing smaller depression[16]. We monitored short-term depression by evoking 10 AP trains at 25 Hz in the presynaptic neuron and recording excitatory postsynaptic currents (EPSCs) in the monosynaptically connected postsynaptic neuron. Peak EPSC amplitudes depressed significantly less for the postsynaptic neuron overexpressing DN-NCad compared to WT-NCad or GFP, and for the neuron knocked down for N-cadherin compared to control scrambled shRNA (Fig. 4d-g). This result is consistent with our observation using the optical quantal analysis of the

reduced p_r of synapses on DN-NCad or N-cadherin knock-down neurons, and it further confirms the role of N-cadherin in regulating the basal neurotransmitter release in *trans*.

We also monitored short-term depression from connected cell pairs in which the postsynaptic neuron was knocked down for β-catenin. In agreement with optical quantal analysis, loss of β-catenin had no effect on the rate of depression of EPSC amplitudes (Suppl Fig. 4f). Therefore, unlike postsynaptic N-cadherin, postsynaptic β-catenin is not required in *trans* to regulate basal p_r.

Effectors of presynaptic regulation by N-cadherin in trans

Because N-cadherin is a homophilic adhesion protein, postsynaptic N-cadherin could influence presynaptic strength by interacting with presynaptic N-cadherin. In this case, interfering with N-cadherin activity presynaptically should mimic the effects of postsynaptic N-cadherin disruption. Unexpectedly, however, synapses between axons overexpressing WT-NCad, DN-NCad, or control GFP, and dendrites of non-transfected neurons showed similar levels of synaptophysin and bassoon when compared to non-transfected axons (synaptophysin and bassoon, respectively, WT-NCad, 1.10 ± 0.09 and 0.98 ± 0.06; DN-NCad, 0.90 ± 0.03 and 0.95 ± 0.06; GFP 0.98 ± 0.05 and 0.98 ± 0.05; P>0.2)(Fig. 5a,b). Moreover, no significant differences in p_r were found for boutons along axons of WT-NCad or DN-NCad neurons relative to control GFP neurons by optical quantal analysis (WT-NCad 0.18 ± 0.03, DN-NCad 0.18 ± 0.03, GFP 0.24 ± 0.03; P>0.2)(Fig. 5c). Such a lack of change in presynaptic release was also supported by paired recordings in which short-term depression was similar whether the presynaptic neuron overexpressed WT-NCad, DN-NCad, or control GFP or was knocked down for N-cadherin or expressed control scrambled shRNA (Fig. 5d-f). Thus, interfering with presynaptic N-cadherin is not sufficient to impair neurotransmitter release in *cis* in contrast to the potent effect of impairing postsynaptic N-cadherin in *trans*. Furthermore, a lack of effect of presynaptically disrupting N-cadherin activity suggests that postsynaptic N-cadherin adjusts presynaptic strength retrogradely by mechanisms that functions independently of presynaptic N-cadherin.

Previous studies have implicated N-cadherin and GluA2 AMPAR subunits in regulating synaptic integrity and function[27,28]; moreover, these two proteins may interact directly to effect their control[9]. We therefore addressed a role for GluA2 in the N-cadherin-dependent transsynaptic regulation of release by examining the effect of impairing postsynaptic N-cadherin activity when GluA2 expression was knocked down by siRNA (Fig. 6). Loss of GluA2 by itself without manipulating N-cadherin activity was sufficient to reduce p_r (scramble siRNA/GFP control 0.29 ± 0.02, GluA2 siRNAs/GFP control 0.18 ± 0.02; P<0.001). Moreover, in the absence of GluA2, overexpressing either WT-NCad or DN-NCad had no additional effect on p_r compared to control GFP (GluA2 siRNA/DN-NCad 0.18 ± 0.01, GluA2 siRNA/WT-NCad 0.16 ± 0.01; P>0.2). Cell pair recordings in which the postsynaptic neuron was knocked down for GluA2, also showed slower short-term depression compared to control neurons in line with decreased p_r (Fig. 6d). Furthermore, in GluA2 knock-down neurons, overexpressing DN-NCad did not further reduce the rate of synaptic depression compared to overexpressing WT-NCad or control GFP, suggesting a lack of further change in p_r upon loss of GluA2. Collectively, both optical quantal analysis and patch clamp recordings indicate that loss of GluA2 occludes the effect of impairing N-cadherin activity on p_r, and thus GluA2 could be a key player in mediating the transsynaptic actions of N-cadherin.

Neuroligin 1 (NLG-1) is another possible interactor of N-cadherin in mediating its presynaptic regulation. A recent study reported of a cooperative role for NLG-1 in controlling SV accumulation at developing synapses[11]. To test for potential involvement for NLG-1 in the N-cadherin-dependent transsynaptic presynaptic modulation, we examined if

impairing postsynaptic N-cadherin altered its synaptic localization. Double immunofluorescence labeling against NLG and vesicular glutamate transporter (VGlut) to identify excitatory synapses where NLG-1 is enriched[29], showed that the synaptic levels of NLG was not significantly different in neurons overexpressing DN-NCad (402 ± 16 AU) or WT-NCad (426 ± 36 AU) compared to GFP control (410 ± 27 AU; P>0.2)(Suppl Fig. 5). A lack of change in the synaptic localization of NLG upon perturbing N-cadherin activity is similar to the lack of change we observe for β-catenin localization in DN-NCad expressing neurons, and this finding is in agreement with the suggestion that NLG-1 could be linked to the N-cadherin/β-catenin complex by interacting with S-SCAM, which binds to β-catenin[11]. Therefore, collectively, these observations are consistent with differential roles played by postsynaptic N-cadherin and β-catenin in regulating presynaptic function. Moreover, because the cooperative facilitatory action of N-cadherin and NLG-1 in clustering of SVs is limited to nascent immature synapses[11], the N-cadherin dependent mechanism we observe could arise following a developmental switch in the transsynaptic control of presynaptic organization.

Postsynaptic N-cadherin and homeostatic plasticity

Homeostatic mechanisms adjust synaptic strength to compensate for changes in network activity and are thought to help maintain neuronal excitation within physiological range[30-32]. Given that interfering with postsynaptic N-cadherin activity is sufficient to impair basal pre and postsynaptic strengths, we wondered if in these synapses homeostatic synaptic plasticity could also be compromised. We thus examined the requirement for postsynaptic N-cadherin activity in the compensatory increase in miniature EPSC (mEPSC) amplitude and frequency that are induced by chronically silencing activity with the Na^+ channel blocker TTX[33-36] (Fig. 7a-c). In agreement with previous observations, without the TTX treatment, overexpressing DN-NCad in postsynaptic neurons decreased mean mEPSC amplitude compared to control GFP neurons, whereas overexpressing WT-NCad had no effect [DN-NCad (P<0.01), 18 ± 1.1 pA; WT-NCad, 22 ± 1.7 pA, GFP 23 ± 2.5 pA][5]. The mean mEPSC frequency was also significantly decreased in DN-NCad neurons [DN-NCad 0.50 ± 0.11 Hz (P<0.01), WT-NCad 0.91 ± 0.14 Hz, GFP 1.03 ± 0.24 Hz], consistent with the reduced synapse density and p_r (above). TTX treatment (1 μM, 36 h) effectively elicited homeostatic synaptic plasticity in control GFP neurons as confirmed by increased mean mEPSC amplitude (23 ± 2.5 to 30 ± 2.0 pA; P<0.05) and frequency (1.03 ± 0.24 to 2.20 ± 0.40 Hz; P<0.05)(Fig. 7a-c; Suppl Fig. 6a,b). Similarly, in neurons overexpressing WT-NCad or DN-NCad, TTX treatment also increased mEPSC amplitude (DN-NCad 18 ± 1.1 to 26 ± 2.7 pA; WT-NCad 22 ± 1.7 to 34 ± 4.9 pA; P<0.05) and frequency (DN-NCad 0.50 ± 0.11 to 1.2 ± 0.25 Hz; WT-NCad 0.91 ± 0.14 to 3.2 ± 1.1 Hz; P<0.05) to extents comparable to the changes observed in control GFP neurons. Collectively, interfering with postsynaptic N-cadherin activity does not apparently compromise the ability of synapses to homeostatically adapt their basal pre- and postsynaptic strengths upon chronic activity blockade.

AMPAR trafficking plays a major role in various forms of synaptic plasticity[32,37-39], and synaptic accumulation of GluA1[40,41] and/or GluA2-containing AMPAR subunits[42-44] could underlie homeostatic scaling of quantal size. Given that N-cadherin interacts with and regulates the trafficking of GluA2-containing AMPARs[9] (although see ref 45), disrupting postsynaptic N-cadherin activity could alter the subunit composition of synaptic AMPARs. To gain insight into possible differential contribution of GluA1 and GluA2 AMPARs to synaptic scaling in neurons compromised for N-cadherin activity, we compared the average mEPSC waveform between TTX and non-treated groups for WT-NCad, DN-NCad and control GFP neurons. Although no changes in mEPSC waveform were detected for any group under basal conditions (90-37% decay time: WT-NCad 4.15 ± 0.23 ms, DN-NCad

4.40 ± 0.25 ms, GFP 4.76 ± 0.27 ms; P>0.2), following TTX treatment, DN-NCad neurons selectively showed a faster mEPSC decay compared to non-drug-treated cells (3.68 ± 0.19 ms; P<0.05); no changes were observed in mEPSC decay for WT-NCad or control GFP neurons following TTX (WT-NCad 4.15 ± 0.37 ms, GFP 4.37 ± 0.33 ms; P>0.2)(Suppl Fig. 6c). The faster decay of mEPSCs in TTX-treated DN-NCad neurons could represent changes in synaptic structure and/or organization associated with impaired postsynaptic N-cadherin activity during homeostatic synaptic plasticity. In one possibility, AMPAR subunit composition could have changed towards dominating GluA1 contribution, as GluA1 currents are larger and decay faster than GluA2 currents[41,46]. In such a case, DN-NCad neurons could have compromised scaling up of GluA2-containing AMPARs following TTX treatment, despite the apparent lack of change in mEPSC amplitude.

To further clarify how N-cadherin might influence the relative contribution of GluA1 and GluA2 to synaptic scaling, we directly monitored surface synaptic GluA1 and GluA2 by live-immunolabeling followed by synapsin I labeling to help identify synapses. Whereas TTX treatment increased surface synaptic GluA2 in WT-NCad (0.9 ± 0.02 to 1.2 ± 0.05 fold) and control GFP neurons (1.0 ± 0.02 to 1.2 ± 0.04 fold), no such increase in surface synaptic GluA2 was detected in DN-NCad cells following TTX (0.8 ± 0.03 to 0.9 ± 0.05 fold)(Fig. 7d). Conversely, surface synaptic GluA1 levels increased in all three conditions after TTX treatment (WT-NCad 1.1 ± 0.04 to 1.3 ± 0.05, DN-NCad 0.9 ± 0.06 to 1.2 ± 0.04, GFP 1.0 ± 0.06 to 1.3 ± 0.07)(Suppl Fig. 6d). Altogether, DN-NCad specifically alters the subunit composition of synaptic AMPARs during homeostatic synaptic scaling, and postsynaptic N-cadherin function is required for scaling up GluA2 but not GluA1.

The mEPSC frequency is a parameter whose changes could indicate altered p_r, although other factors such as synapse density and postsynaptic silencing could also contribute. Therefore, to corroborate the mEPSC frequency analysis in investigating postsynaptic N-cadherin's role in homeostatic adaptation of presynaptic release, we used the method of optical quantal analysis to estimate p_r and compared the effect of TTX treatment at synapses received by neurons overexpressing WT-NCad, DN-NCad or control GFP (Fig. 7e). At boutons on control GFP neurons, TTX significantly increased p_r relative to non-drug-treated cells (0.34 ± 0.04 to 0.54 ± 0.05; P<0.05). TTX treatment also increased p_r at synapses on WT-NCad (0.33 ± 0.03 to 0.60 ± 0.05; P<0.01) and DN-NCad neurons (0.19 ± 0.01 to 0.34 ± 0.07; P<0.05) to an extent comparable to the p_r increase observed in control GFP neurons. Moreover, neurons overexpressing N-cadherin ΔC mutant lacking the β-catenin binding region, also showed a similar increase in p_r relative to control GFP neurons following TTX treatment [0.22 ± .0.1 to 0.39 ± 0.04 (P<0.001) and 0.22 ± 0.04 to 0.40 ± 0.03 (P<0.01) for NCad ΔC and control GFP, respectively](Fig. 7f). Postsynaptic N-cadherin activity, including its interaction to β-catenin, is therefore not required for the homeostatic upregulation of p_r induced by chronic activity block.

β-catenin in homeostatic regulation of release probability

Our experiments show that, surprisingly, postsynaptic N-cadherin and β-catenin have differential effects on presynaptic efficacy and organization in *trans*: contrary to impairing postsynaptic N-cadherin activity, ablating postsynaptic β-catenin does not affect the basal p_r and the levels of synaptophysin and bassoon. As N-cadherin ΔC mutant unable to interact with β-catenin, did not block TTX-dependent increase in p_r, we wondered if homeostatic upregulation of presynaptic strength could also differentially involve postsynaptic N-cadherin and β-catenin in *trans.* We therefore analyzed p_r with or without TTX treatment at synapses where β-catenin was knocked down specifically in postsynaptic neurons using β-catenin floxed mice cultures (see above). Whereas in control GFP neurons TTX treatment significantly increased p_r relative to non-TTX-treated cells (0.25 ± 0.02 to 0.39 ± 0.04; P<0.05), boutons on Cre-IRES-GFP neurons did not up-regulate p_r relative to untreated cells

(0.28 ± 0.02 to 0.26 ± 0.04; P>0.2)(Fig. 7g). Pair-wise patch clamp recordings were also carried out in β-catenin floxed cultures where the postsynaptic neuron expressed either Cre or control GFP. TTX treatment increased the rate of synaptic depression to repetitive stimulation only in control GFP and not in β-catenin knock-down neurons expressing Cre (Suppl Fig. 4f), in agreement with a block of upregulation of p_r upon loss of postsynaptic β-catenin. Therefore, postsynaptic β-catenin is required in *trans* for the homeostatic upregulation of p_r induced by chronic activity silencing, whereas postsynaptic N-cadherin activity is dispensable under parallel conditions.

β-catenin has a number of protein interaction domains. In particular, the central armadillo repeat region mediates binding to N-cadherin and to TCF/LEF transcription factors, while the PDZ binding motif in the C-terminal domain interacts with PDZ proteins such as S-SCAM[11]. To determine whether these two regions played a role in β-catenin-dependent homeostatic adaptation of presynaptic release, we tested the effect of overexpressing β-catenin deletion mutants lacking the armadillo repeat region (ΔARM) or the PDZ binding motif (ΔPDZ)[5] on p_r by optical quantal analysis with or without TTX treatment (Fig. 7h,i). As expected from the lack of effect of postsynaptic β-catenin knock-down on basal p_r, we found no change in p_r in neurons overexpressing either β-catenin ΔPDZ or ΔARM mutant compared to control neurons under basal conditions. Following TTX treatment, whereas β-catenin ΔPDZ neurons increased p_r (0.28 ± 0.04 to 0.50 ± 0.08; P<0.01) similarly to control neurons (0.23 ± 0.03 to 0.53 ± 0.04; P<0.001), no such increase was observed for β-catenin ΔARM neurons (0.27 ± 0.04 to 0.34 ± 0.03). Therefore, β-catenin interactions via the armadillo repeat region but not the PDZ binding domain are important for presynaptic homeostatic adaptation. Because the association between β-catenin and N-cadherin is dispensable for upregulating p_r upon activity silencing (Fig. 7f), transcriptional regulation by β-catenin in postsynaptic neurons is likely to be a key component of the mechanism of retrograde homeostatic modulation.

Postsynaptic N-cadherin affects endocytosis in trans

Our finding that the loss of postsynaptic N-cadherin activity compromised p_r in *trans* was based on the optical quantal analysis, which relied on exo-endocytic coupling of SVs to monitor the FM-dye uptake. Thus, the observed reduction in presynaptic efficacy could be due to alterations in SV exocytosis, endocytosis or both. To clarify this point we examined the time course of exocytosis and endocytosis separately at boutons on neurons overexpressing DN-NCad or control GFP (Fig. 8). First, we analyzed exocytosis by preloading the entire recycling pool with FM4-64 and then monitoring dye destaining kinetics during 2 Hz stimulation. Single exponential fits showed no differences in the rate of fluorescence dye loss between synapses expressing the DN-NCad or GFP postsynaptically (P>0.2; decay time constant: 108 ± 2.6 s vs. 113 ± 3.4 s for control vs. DN-NCad, respectively). Therefore, postsynaptic DN-NCad is not sufficient to transsynaptically compromise SVs exocytosis *per se*.

Next, we measured the kinetics of endocytosis by determining the amount of FM dye uptake at different time intervals (Δt) after the end of a 300 AP stimulus train. In this assay, progressively fewer endocytic events are caught with increasing Δt, thereby leading to lesser dye incorporation into SVs, and the rate of reduction in the amount of dye uptake is a measure of endocytosis rate[47]. Boutons on DN-NCad neurons showed a significantly slower decline in FM dye uptake compared to control boutons, with half maximal uptake occurring within ~32 s of the end of stimulation for DN-NCad expressing neurons compared to ~18 s for control boutons. Therefore, interfering with postsynaptic N-cadherin activity induces a 2-fold reduction in the endocytosis rate. These data indicate that postsynaptic N-cadherin controls presynaptic efficacy transsynaptically by targeting SV endocytosis.

DISCUSSION

We have systematically studied the transsynaptic regulation of presynaptic efficacy by N-cadherin. Two independent assays for monitoring SV dynamics, FM dyes and anti-synaptotagmin I luminal domain antibody confirm that interfering with postsynaptic N-cadherin activity reduces transmitter release in *trans,* which is also supported by slowed short-term synaptic depression. Recently, pHluorin-tagged vesicle proteins have been popularly used to monitor SV recycling, particularly in cultured neurons where one can follow single quantal events. We have however not used genetically encoded vesicle probes because of the very low yield of finding synapses that presynaptically express the optical probe and postsynaptically manipulated for N-cadherin or β-catenin expression.

In contrast to overexpressing DN-NCad or knocking down endogenous N-cadherin, overexpressing WT-NCad in postsynaptic neurons produced no evident changes in the presynaptic organization and release in *trans*. The cytoplasmic domain of N-cadherin interacts with a variety of proteins such as β-catenin and p120catenin family members[48]. If the presynaptic modulation by postsynaptic N-cadherin is facilitated or occurs via N-cadherin interacting proteins, then the abundance and/or activity of the interacting proteins could be limiting, and excess postsynaptic N-cadherin without a binding partner might be ineffective in exerting transsynaptic control. Notably, overexpressing DN-Ncad, WT-NCad or knocking down endogenous N-cadherin along axons has no effect on presynaptic synaptophysin and bassoon levels and p_r. Therefore, presynaptic N-cadherin seems dispensable for controlling the presynaptic organization and function, further highlighting the importance of postsynaptic N-cadherin interacting proteins for mediating the presynaptic changes.

Our study reveals GluA2 as a potential N-cadherin interactor in the transsynaptic mechanism that controls p_r. This is in agreement with previous reports of a role for GluA2 in regulating synapse integrity and function[27,28], which may involve a direct interaction between N-cadherin and GluA2[9]. However, despite the apparent requirement for GluA2 in regulating p_r, the decreased synaptic GluA2 observed with impairing postsynaptic N-cadherin activity or β-catenin accompanies a reduced p_r only with N-cadherin interference but not with β-catenin loss. Such a lack of change in p_r in β-catenin knock down neurons could reflect the difference in the way in which GluA2 is reduced compared to impairing N-cadherin activity. That is, the remaining GluA2 in β-catenin knock down neurons might still be complexed to and/or interacting with N-cadherin in sufficient numbers to enable presynaptic control.

The reduced p_r upon impairing postsynaptic N-cadherin activity is associated with a prominent slowing of endocytosis without an appreciable change in exocytosis. The slowed endocytosis could at least partly account for the observed decreases in the total SV number and the recycling vesicle pool size. How might postsynaptic N-cadherin affect presynaptic endocytosis in *trans*? In one possibility, postsynaptic N-cadherin interactors could generate a diffusible retrograde signal or modify other adhesion protein-dependent signaling system spanning the synaptic cleft[49] to target the endocytosis machinery. Alternatively, the endocytosis defect could represent a secondary consequence of some synaptic structural change, for example, implemented by N-cadherin interaction with other adhesion systems[11,22]. Whereas unaltered mEPSC waveform by DN-NCad overexpression is suggestive of a lack of change in synaptic cleft geometry[46], impaired postsynaptic N-cadherin activity could subtly introduce mechanical changes to the presynaptic membrane and affect exo-endocytic coupling so as to significantly compromise endocytosis. Moreover, our data do not rule out a potential effect on exocytosis that may have been too small to be detected by the FM dye destaining experiments. In dual patch clamp recordings, the reduced

synaptic depression in DN-NCad neurons relative to controls is detectable within 80 ms (Fig. 4e), which is much faster than the time scale of endocytosis that occurs in seconds. Further studies are needed to clarify the mechanism by which SV endocytosis defect arises by impairing postsynaptic N-cadherin activity.

We find that postsynaptic N-cadherin and β-catenin differentially affect presynaptic efficacy in *trans*. Whereas postsynaptic N-cadherin is required for basal p_r regulation but not for homeostatic presynaptic adaptation, postsynaptic β-catenin is not apparently required for controlling the basal p_r but is needed for the homeostatic resetting of p_r. Such differential requirements are surprising given the robust link between N-cadherin and β-catenin[48]. Nevertheless, our findings are in line with a suggestion that excitatory synapses contain a pool of N-cadherin that does not colocalize with β-catenin and respond to synaptic activity in a β-catenin-independent manner[50]. Interestingly, the differential effects of interfering with postsynaptic N-cadherin and β-catenin also extend to synapse density. Postsynaptic DN-NCad overexpression reduces synapse density[1] and mEPSC frequency (Fig. 7c), indicating a role for postsynaptic N-cadherin in synapse formation or stabilization. In contrast, ablating β-catenin in postsynaptic neurons does not alter synapse density or mEPSC frequency[5]. Based on the requirements for N-cadherin in setting the basal p_r, and in parallel, for synapse formation or maintenance, it is tempting to speculate that the level of basal p_r associated with a given synapse is set at the time of synapse formation and may be inherent to the manner in which synapses are formed and maintained. In contrast, the homeostatic adjustment of the gain of p_r, which is dependent on β-catenin and possibly transcriptional modulation, is uncoupled from regulation of synapse stability thereby allowing for an additional level of control. The molecular mechanism by which postsynaptic β-catenin adjusts the presynaptic p_r retrogradely according to the level of network activity is the aim of future work.

METHODS

DNA constructs

The full length N-cadherin (NC), dominant-negative N-cadherin (DN), N-cadherin C-terminal deletion (NC-ΔC), β-catenin ΔPDZ, β-catenin ΔARM and Cre-pIRES2-EGFP constructs were as previously described[5]. A commercially available shRNA against N-cadherin and control (Mission shRNA; Sigma-Aldrich) were used in this study. GluA2 siRNA and control was kindly provided by M. Passafaro.

Neuronal cell cultures and transfection

Animal care and use protocols were approved by the Home Office (UK). Dissociated hippocampal cultures were prepared from P0-P1 rats or β-catenin-floxed mice (provided by R. Kemler, Max-Planck Institute of Immunology, Freiburg, Germany) and plated at low density onto an astrocyte feeder layer. The cultures were maintained as described previously[17]. Neurons were transfected at DIV 10 using a Ca^{2+} phosphate protocol[42]. β-catenin ΔPDZ, β-catenin ΔARM, NC shRNA and scrambled shRNA constructs were cotransfected with a GFP-expressing plasmid. Cultures were used for experiments at DIV 12-14. Where noted, cells were treated with TTX (1 μM) for 36 h before experiments.

Live-labeling and immunocytochemistry

Anti-synaptotagmin1 antibody uptake experiments were performed by delivering 900 APs to neurons by field stimulation in the presence of a rabbit polyclonal antibody against the luminal domain of synaptotagmin-1 (1:100, Synaptic Systems) diluted in normal HEPES-buffered bath solution (EBS) containing (mM): 137 NaCl, 5 KCl, 2 $CaCl_2$, 2 $MgCl_2$, 10 D-glucose, 5 HEPES, 0.1 picrotoxin, 20 μM 6-cyano-7-nitroquinoxaline-2,3-dione (CNQX)

and 50 μM D-2-amino-5-phosphonovaleric acid (AP5) at room temperature. After 2 washes with normal EBS, the cells were fixed in 4% paraformaldehyde in PBS. Surface labeling for GluA1 and GluA2 was carried out using rabbit polyclonal anti-GluA1 (1:10, Calbiochem) or mouse monoclonal anti-GluA2 monoclonal antibody (1:200, Chemicon) in culture medium for 15 min at 37°C, rinsed with EBS followed by fixation in 4% paraformaldehyde as above.

In all experiments, after fixation cells were permeabilized with 0.1% Triton X-100 and blocked in PBS containing 0.2M glycine, 10% fetal bovine serum and 0.1% Triton X-100 for 1 h at room temperature. Primary antibodies were added in blocking solution and incubated for 2 h at room temperature. The following primary antibodies and dilutions were used: rabbit anti-GluA2/3 (1:250, Chemicon), mouse anti-bassoon (1:1000, StressGen Biotech), rabbit anti-synapsin (1:2000, Synaptic Systems), mouse anti-synapsin (1:1000, Synaptic Systems), mouse anti-synaptophysin (1:500, Synaptic Systems), rabbit anti-synaptophysin (1:500, Synaptic Systems), chicken anti-GFP (1:1000, Abcam), mouse anti-β-catenin (1:250, BD Biosciences), rabbit anti-Tau (1:800, Abcam), mouse anti-neurofilament H (1:500, Millipore), mouse anti-neuroligin (1:250, Synaptic System) and rabbit anti-vGlut1 (1:2000, Synaptic Systems). After 3 washes in PBS, neurons were incubated with secondary fluorescently-conjugated antibodies [Alexafluor 568 (Invitrogen), Cy2 or Cy5 (Jackson Laboratories)].

Correlative transmission electron microscopy

After identifying transfected cells, fluorescence and brightfield images of the regions of interest were acquired at different magnifications using an Olympus BX50WI upright epifluorescence microscope. Cells were fixed in 2% paraformaldehyde/2% glutaraldehyde (both EM grade from TAAB) in 0.1 M sodium cacodylate buffer for 30 min at room temperature. Samples were then secondarily fixed in 1% osmium tetroxide/1.5% potassium ferricyanide for 1 h at 4°C. Following washes in 0.1% sodium cacodylate, coverslips were incubated in 1% tannic acid in 0.5% sodium cacodylate at room temperature for 45 min. Further washes in 0.5% sodium cacodylate were followed by a final wash in distilled water, before the samples underwent dehydration by sequential short incubations in 70%, and 90% ethanol, and then two longer incubations in 100% ethanol. Coverslips were transferred to a 1:1 mix of propylene oxide and Epon resin (TAAB) for 90 min, then 100% epon for two further 90 min incubations. Finally coverslips were inverted onto pre polymerized epon stubs ensuring that the area of interest was safely on the stub itself, and samples were polymerized by baking at 60°C overnight. Coverslips were removed by rapid immersion of the samples in liquid nitrogen. The cells of interest were found on the block surface using the light microscopy images. Small block faces were trimmed and then serial 70 nm ultrathin sections cut with a diamond knife. Ribbons of sections were collected on formvar coated slot grids, and stained using Reynolds lead citrate prior to imaging. Samples were imaged using an FEI Tecnai G2 Spirit transmission electron microscope using an Olympus SIS Morada CCD camera. Asymmetric (excitatory) synapses were identified by a thick PSD and presence of round-shaped vesicles in presynaptic terminals. Per single section, the total number of SVs and the number of docked vesicles in direct contact with the presynaptic terminal at the active zone defined by the postsynaptic apposition to the PSD were counted.

FM Imaging

Epifluorescence images were acquired on an Olympus BX50WI upright microscope using a cooled CCD camera (Princeton Instruments). SVs were labeled by 7, 40 or 900 APs delivered by field stimulation in a custom-made chamber in the presence of FM4-64 (15 μM, Invitrogen); 45 s after the end of stimulation the excess dye was washed with EBS containing 1 mM Advasep-7 (Biotium) for 1 min and then rinsed with EBS for 10 min. Images were acquired every 30 s before and after unloading stimulation by 600 APs at 20

Hz for three rounds with 15 s intervals or 900 APs at 10 Hz. The remaining signal was taken as background. Experiments were carried out in normal EBS except for experiments monitoring extracellular Ca^{2+} sensitivity (Fig. 4C) where the FM dye loading was performed in EBS containing 2 or 5 mM Ca^{2+}. FM4-64 dye destaining kinetics was monitored during unloading stimulation of 600 APs at 2 Hz. In pulse-chase FM4-64 experiments, the cultures were stimulated by 300 APs at 10 Hz and exposed to the dye for 1 min after a variable delay time from the end of stimulation. All experiments were performed at room temperature.

Image Analysis

Transfected neurons were quantified from at least two independent experiments for each construct. The number of neurons or puncta used for quantification is indicated in the figures. Images were analyzed using MetaMorph imaging software (Universal Imaging Corporation, West Chester, PA). To quantify signals associated with pre and postsynaptic markers, background signal (nonpunctate region) was subtracted and integrated fluorescence intensity of individual puncta was measured and averaged per neuron, and the ratio between values in transfected cells with those in untransfected neurons in the same coverslip was determined. The number of neurons from which the ratio of mean values was averaged to calculate the population mean is indicated in Figure legends. For measurements of total synaptic GluA2/3 and surface synaptic GluA1 and GluA2 levels, we restricted our analysis to synapses that displayed partial or completely overlapping signals between postsynaptic receptors and presynaptic markers.

To quantify FM4-64 fluorescence, background signals were subtracted, and integrated fluorescence intensities of individual puncta were measured using MetaMorph imaging software (Universal Imaging Corporation, West Chester, PA). Release probability was estimated by optical quantal analysis as previously described with slight modifications[24]. FM4-64 was loaded by 40 APs at 1 Hz and p_r was $F/q/40$, where F was integrated fluorescence intensity of the FM4-64 puncta, and q was the quantal FM4-64 fluorescence measured from sister coverslips on the same day (in which FM was loaded by 7 APs at 0.5 Hz)[13, 23, 24]. Release probability was calculated for each synapse and averaged per neuron.

Electrophysiology

Whole cell patch-clamp recordings were carried out from culture chamber placed on the stage of an Olympus IX70 inverted microscope at room temperature and using Axopatch 200B or multiclamp amplifiers (Axon Instruments). Transfected cells were identified using standard epifluorescence. The recording chamber was continuously perfused with an aCSF containing (mM): 130 NaCl, 2.5 KCl, 2.2 $CaCl_2$, 1.5 $MgCl_2$, 10 D-glucose, 10 HEPES, 0.1 picrotoxin (pH 7.35, osmolarity adjusted to 290 mOsm). 0.5μM TTX was added to block sodium channels when recording mEPSCs. The intracellular solution contained (mM): 100 Kgluconate, 17 KCl, 5 NaCl, 5 $MgCl_2$, 10 HEPES, 0.5 EGTA, 4 $ATPK_2$, 0.5 GTPNa (pH 7.3, osmolarity adjusted to 280 mOsm). Recorded neurons were held under voltage clamp at −70 mV and series resistance was left uncompensated. Pipette resistance was 3-5 MΩ and only cells with stable resting potential of < −50 mV and series resistance of < 20 MΩ were analyzed.

For paired recordings, monosynaptic connections were identified by a short latency (< 10 ms). Short-term plasticity was monitored by evoking 10 APs at 25 Hz with brief depolarizations (1 ms, 100 mV) of the presynaptic neuron. The amplitude of the evoked post-synaptic responses was measured using the Clampfit software (Axon Instruments).

mEPSCs were recorded over a period of 5 – 10 min, and recordings were filtered at 2kHz and sampled at 10kHz using the pClamp software (Axon Instruments). Amplitude, frequency and decay time (90-37% of the peak amplitude) of the events were analyzed using mini analysis software (Synaptosoft). The detection threshold was set at −6 pA. Cells with a noisy or unstable baseline were discarded. Raw data was inspected to eliminate any false event.

Statistics

Statistical significance was determined by the two-tailed Student *t* test or one-way ANOVA. The Mann-Whitney test was used when criteria for normality were not met. All data are shown as the mean ± SEM. Statistical significance was assumed when $P < 0.05$. In figures, $^{*}P < 0.05$, $^{**}P < 0.01$, and $^{***}P < 0.001$.

Supplementary Material

Refer to Web version on PubMed Central for supplementary material.

Acknowledgments

We thank Rolf Kemler for β-catenin floxed mice, Takashi Okuda and Maria Passafaro for sharing plasmids, David Elliott for expert technical assistance and the members of the Goda lab for helpful discussions. This work was supported by the MRC, the EU 7th Framework Program EUROSPIN project, and the RIKEN Brain Science Institute.

REFERENCES

1. Togashi H, et al. Interneurite affinity is regulated by heterophilic nectin interactions in concert with the cadherin machinery. The Journal of cell biology. 2006; 174:141–151. [PubMed: 16801389]
2. Abe K, Chisaka O, Van Roy F, Takeichi M. Stability of dendritic spines and synaptic contacts is controlled by alpha N-catenin. Nature neuroscience. 2004; 7:357–363.
3. Bamji SX, et al. Role of beta-catenin in synaptic vesicle localization and presynaptic assembly. Neuron. 2003; 40:719–731. [PubMed: 14622577]
4. Murase S, Mosser E, Schuman EM. Depolarization drives beta-Catenin into neuronal spines promoting changes in synaptic structure and function. Neuron. 2002; 35:91–105. [PubMed: 12123611]
5. Okuda T, Yu LM, Cingolani LA, Kemler R, Goda Y. beta-Catenin regulates excitatory postsynaptic strength at hippocampal synapses. Proceedings of the National Academy of Sciences of the United States of America. 2007; 104:13479–13484. [PubMed: 17679699]
6. Tang L, Hung CP, Schuman EM. A role for the cadherin family of cell adhesion molecules in hippocampal long-term potentiation. Neuron. 1998; 20:1165–1175. [PubMed: 9655504]
7. Bozdagi O, et al. Persistence of coordinated long-term potentiation and dendritic spine enlargement at mature hippocampal CA1 synapses requires N-cadherin. J Neurosci. 2010; 30:9984–9989. [PubMed: 20668183]
8. Mendez P, De Roo M, Poglia L, Klauser P, Muller D. N-cadherin mediates plasticity-induced long-term spine stabilization. The Journal of cell biology. 2010; 189:589–600. [PubMed: 20440002]
9. Saglietti L, et al. Extracellular interactions between GluR2 and N-cadherin in spine regulation. Neuron. 2007; 54:461–477. [PubMed: 17481398]
10. Jungling K, et al. N-cadherin transsynaptically regulates short-term plasticity at glutamatergic synapses in embryonic stem cell-derived neurons. J Neurosci. 2006; 26:6968–6978. [PubMed: 16807326]
11. Stan A, et al. Essential cooperation of N-cadherin and neuroligin-1 in the transsynaptic control of vesicle accumulation. Proceedings of the National Academy of Sciences of the United States of America. 2010; 107:11116–11121. [PubMed: 20534458]

12. Hessler NA, Shirke AM, Malinow R. The probability of transmitter release at a mammalian central synapse. Nature. 1993; 366:569–572. [PubMed: 7902955]
13. Murthy VN, Sejnowski TJ, Stevens CF. Heterogeneous release properties of visualized individual hippocampal synapses. Neuron. 1997; 18:599–612. [PubMed: 9136769]
14. Rosenmund C, Clements JD, Westbrook GL. Nonuniform probability of glutamate release at a hippocampal synapse. Science (New York, N.Y. 1993; 262:754–757.
15. Pang ZP, Sudhof TC. Cell biology of Ca2+-triggered exocytosis. Current opinion in cell biology. 2010; 22:496–505. [PubMed: 20561775]
16. Zucker RS, Regehr WG. Short-term synaptic plasticity. Annual review of physiology. 2002; 64:355–405.
17. Branco T, Staras K, Darcy KJ, Goda Y. Local dendritic activity sets release probability at hippocampal synapses. Neuron. 2008; 59:475–485. [PubMed: 18701072]
18. Frank CA, Kennedy MJ, Goold CP, Marek KW, Davis GW. Mechanisms underlying the rapid induction and sustained expression of synaptic homeostasis. Neuron. 2006; 52:663–677. [PubMed: 17114050]
19. Jakawich SK, et al. Local presynaptic activity gates homeostatic changes in presynaptic function driven by dendritic BDNF synthesis. Neuron. 2010; 68:1143–1158. [PubMed: 21172615]
20. Lindskog M, et al. Postsynaptic GluA1 enables acute retrograde enhancement of presynaptic function to coordinate adaptation to synaptic inactivity. Proceedings of the National Academy of Sciences of the United States of America. 2010
21. Frank CA, Pielage J, Davis GW. A presynaptic homeostatic signaling system composed of the Eph receptor, ephexin, Cdc42, and CaV2.1 calcium channels. Neuron. 2009; 61:556–569. [PubMed: 19249276]
22. Futai K, et al. Retrograde modulation of presynaptic release probability through signaling mediated by PSD-95-neuroligin. Nature neuroscience. 2007; 10:186–195.
23. Ryan TA, Reuter H, Smith SJ. Optical detection of a quantal presynaptic membrane turnover. Nature. 1997; 388:478–482. [PubMed: 9242407]
24. Tokuoka H, Goda Y. Activity-dependent coordination of presynaptic release probability and postsynaptic GluR2 abundance at single synapses. Proceedings of the National Academy of Sciences of the United States of America. 2008; 105:14656–14661. [PubMed: 18794522]
25. Takeichi M. Cadherins: a molecular family important in selective cell-cell adhesion. Annual review of biochemistry. 1990; 59:237–252.
26. Brault V, et al. Inactivation of the beta-catenin gene by Wnt1-Cre-mediated deletion results in dramatic brain malformation and failure of craniofacial development. Development (Cambridge, England). 2001; 128:1253–1264.
27. Passafaro M, Nakagawa T, Sala C, Sheng M. Induction of dendritic spines by an extracellular domain of AMPA receptor subunit GluR2. Nature. 2003; 424:677–681. [PubMed: 12904794]
28. Ripley B, Otto S, Tiglio K, Williams ME, Ghosh A. Regulation of synaptic stability by AMPA receptor reverse signaling. Proceedings of the National Academy of Sciences of the United States of America. 2011; 108:367–372. [PubMed: 21173224]
29. Song JY, Ichtchenko K, Sudhof TC, Brose N. Neuroligin 1 is a postsynaptic cell-adhesion molecule of excitatory synapses. Proceedings of the National Academy of Sciences of the United States of America. 1999; 96:1100–1105. [PubMed: 9927700]
30. Burrone J, Murthy VN. Synaptic gain control and homeostasis. Current opinion in neurobiology. 2003; 13:560–567. [PubMed: 14630218]
31. Pozo K, Goda Y. Unraveling mechanisms of homeostatic synaptic plasticity. Neuron. 2010; 66:337–351. [PubMed: 20471348]
32. Turrigiano GG. The self-tuning neuron: synaptic scaling of excitatory synapses. Cell. 2008; 135:422–435. [PubMed: 18984155]
33. Burrone J, O'Byrne M, Murthy VN. Multiple forms of synaptic plasticity triggered by selective suppression of activity in individual neurons. Nature. 2002; 420:414–418. [PubMed: 12459783]

34. Han EB, Stevens CF. Development regulates a switch between post- and presynaptic strengthening in response to activity deprivation. Proceedings of the National Academy of Sciences of the United States of America. 2009; 106:10817–10822. [PubMed: 19509338]
35. Nakayama K, Kiyosue K, Taguchi T. Diminished neuronal activity increases neuron-neuron connectivity underlying silent synapse formation and the rapid conversion of silent to functional synapses. J Neurosci. 2005; 25:4040–4051. [PubMed: 15843606]
36. Wierenga CJ, Walsh MF, Turrigiano GG. Temporal regulation of the expression locus of homeostatic plasticity. Journal of neurophysiology. 2006; 96:2127–2133. [PubMed: 16760351]
37. Bredt DS, Nicoll RA. AMPA receptor trafficking at excitatory synapses. Neuron. 2003; 40:361–379. [PubMed: 14556714]
38. Newpher TM, Ehlers MD. Glutamate receptor dynamics in dendritic microdomains. Neuron. 2008; 58:472–497. [PubMed: 18498731]
39. Sheng M, Hoogenraad CC. The postsynaptic architecture of excitatory synapses: a more quantitative view. Annual review of biochemistry. 2007; 76:823–847.
40. Sutton MA, Schuman EM. Dendritic protein synthesis, synaptic plasticity, and memory. Cell. 2006; 127:49–58. [PubMed: 17018276]
41. Thiagarajan TC, Lindskog M, Tsien RW. Adaptation to synaptic inactivity in hippocampal neurons. Neuron. 2005; 47:725–737. [PubMed: 16129401]
42. Cingolani LA, et al. Activity-dependent regulation of synaptic AMPA receptor composition and abundance by beta3 integrins. Neuron. 2008; 58:749–762. [PubMed: 18549786]
43. Gainey MA, Hurvitz-Wolff JR, Lambo ME, Turrigiano GG. Synaptic scaling requires the GluR2 subunit of the AMPA receptor. J Neurosci. 2009; 29:6479–6489. [PubMed: 19458219]
44. Wierenga CJ, Ibata K, Turrigiano GG. Postsynaptic expression of homeostatic plasticity at neocortical synapses. J Neurosci. 2005; 25:2895–2905. [PubMed: 15772349]
45. Nuriya M, Huganir RL. Regulation of AMPA receptor trafficking by N-cadherin. Journal of neurochemistry. 2006; 97:652–661. [PubMed: 16515543]
46. Cathala L, Holderith NB, Nusser Z, DiGregorio DA, Cull-Candy SG. Changes in synaptic structure underlie the developmental speeding of AMPA receptor-mediated EPSCs. Nature neuroscience. 2005; 8:1310–1318.
47. Ryan TA, et al. The kinetics of SV recycling measured at single presynaptic boutons. Neuron. 1993; 11:713–724. [PubMed: 8398156]
48. Arikkath J, Reichardt LF. Cadherins and catenins at synapses: roles in synaptogenesis and synaptic plasticity. Trends in neurosciences. 2008; 31:487–494. [PubMed: 18684518]
49. Gottmann K. Transsynaptic modulation of the synaptic vesicle cycle by cell-adhesion molecules. Journal of neuroscience research. 2008; 86:223–232. [PubMed: 17787017]
50. Tanaka H, et al. Molecular modification of N-cadherin in response to synaptic activity. Neuron. 2000; 25:93–107. [PubMed: 10707975]

Europe PMC Funders Author Manuscripts

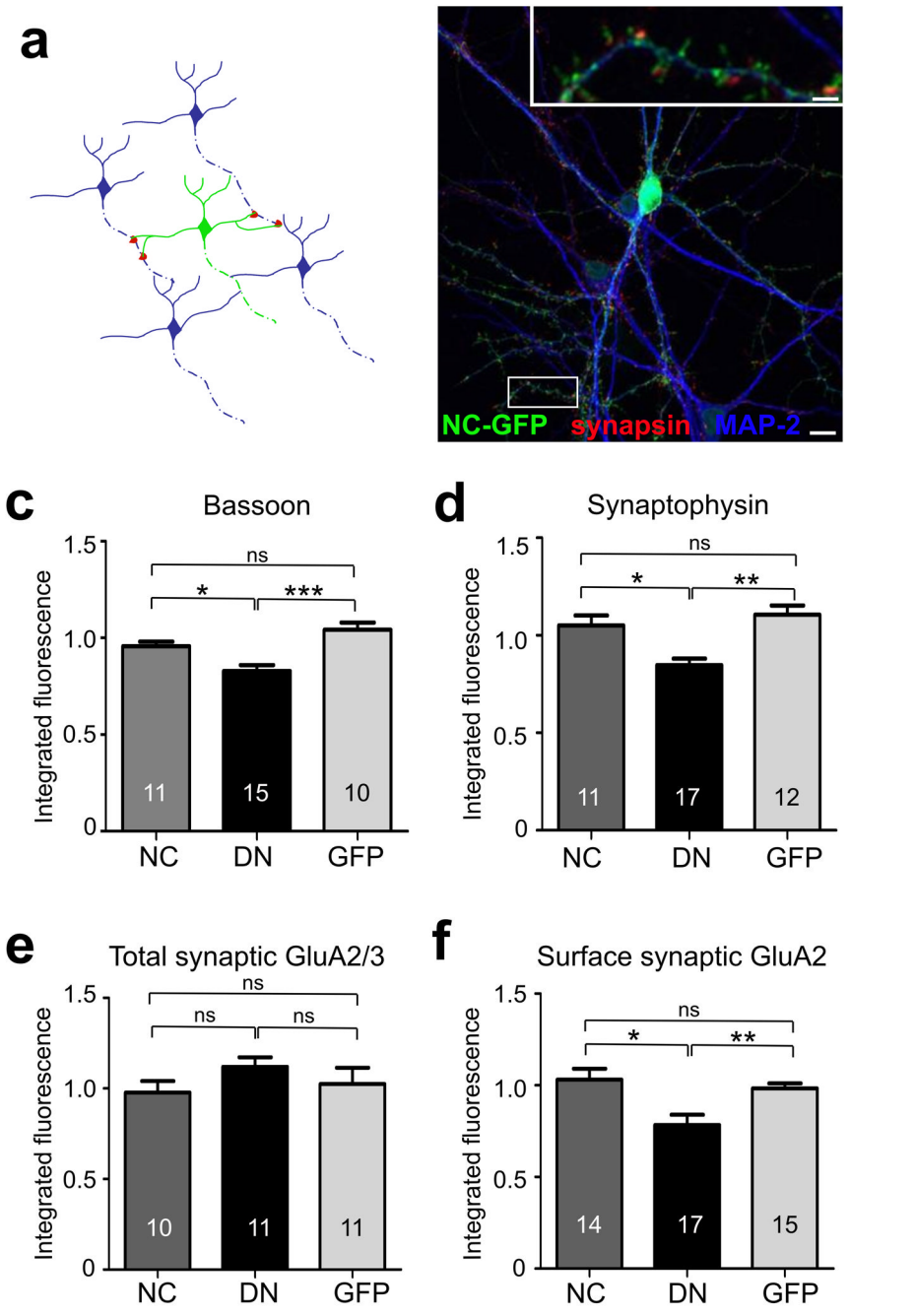

Figure 1. Postsynaptic expression of DN-NCad decreases the levels of presynaptic proteins

a, Experimental scheme: due to a low transfection efficiency a neuron expressing a construct of interest receives inputs mostly from untransfected cells. **b,** Example image of a hippocampal neuron expressing GFP-tagged WT-NCad and double labeled for synapsin and MAP2. **c-f,** Summary of integrated immunofluorescence puncta intensity of labeling against pre- and postsynaptic protein in cells postsynaptically expressing WT-NCad (NC), DN-NCad (DN) or GFP. Synaptic puncta were identified by double labeling for bassoon or synaptophysin and GluA2/3, or for synapsin and surface GluA2. Bars show mean ± SEM for each group relative to untransfected neighboring neurons in the same field of view. The number of neurons is indicated in bars; *P<0.05, **P<0.01, ***P<0.001, ns denotes no

statistically significant difference, one way ANOVA followed by Tukey's test. Scale bar, 20 μm; inset 3 μm.

Europe PMC Funders Author Manuscripts

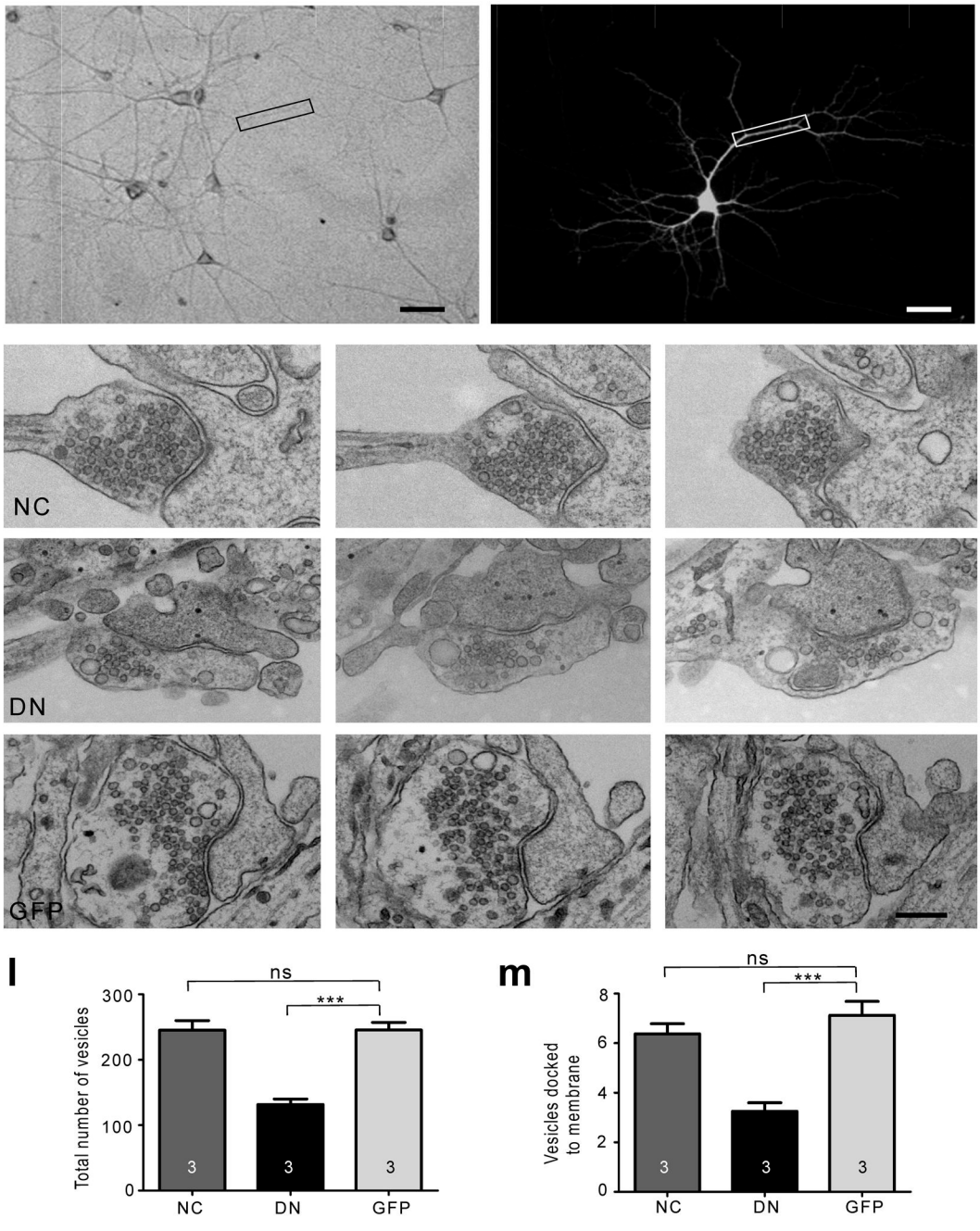

Figure 2. Ultrastructural analysis of SV distribution

a-b, Brightfield and fluorescence images of a representative transfected hippocampal neuron used for correlative light and EM analysis. Scale bar, 50 μm. **c-k**, Three consecutive serial sections of example synapses formed onto dendrites expressing WT-NCad (NC)**,** DN-NCad (DN) or GFP. **l, m**, Summary of the total number of vesicles (l) and the number of vesicles docked to the active zone (m). Bars show mean ± SEM. The number of neurons used is shown in bars; n=23, 16, and 24 synapses for NC, DN and GFP, respectively; one way ANOVA followed by Tukey's test. *P<0.05, **P<0.01, ***P<0.001. ns, no statistically significant difference. Scale bar, 100 nm.

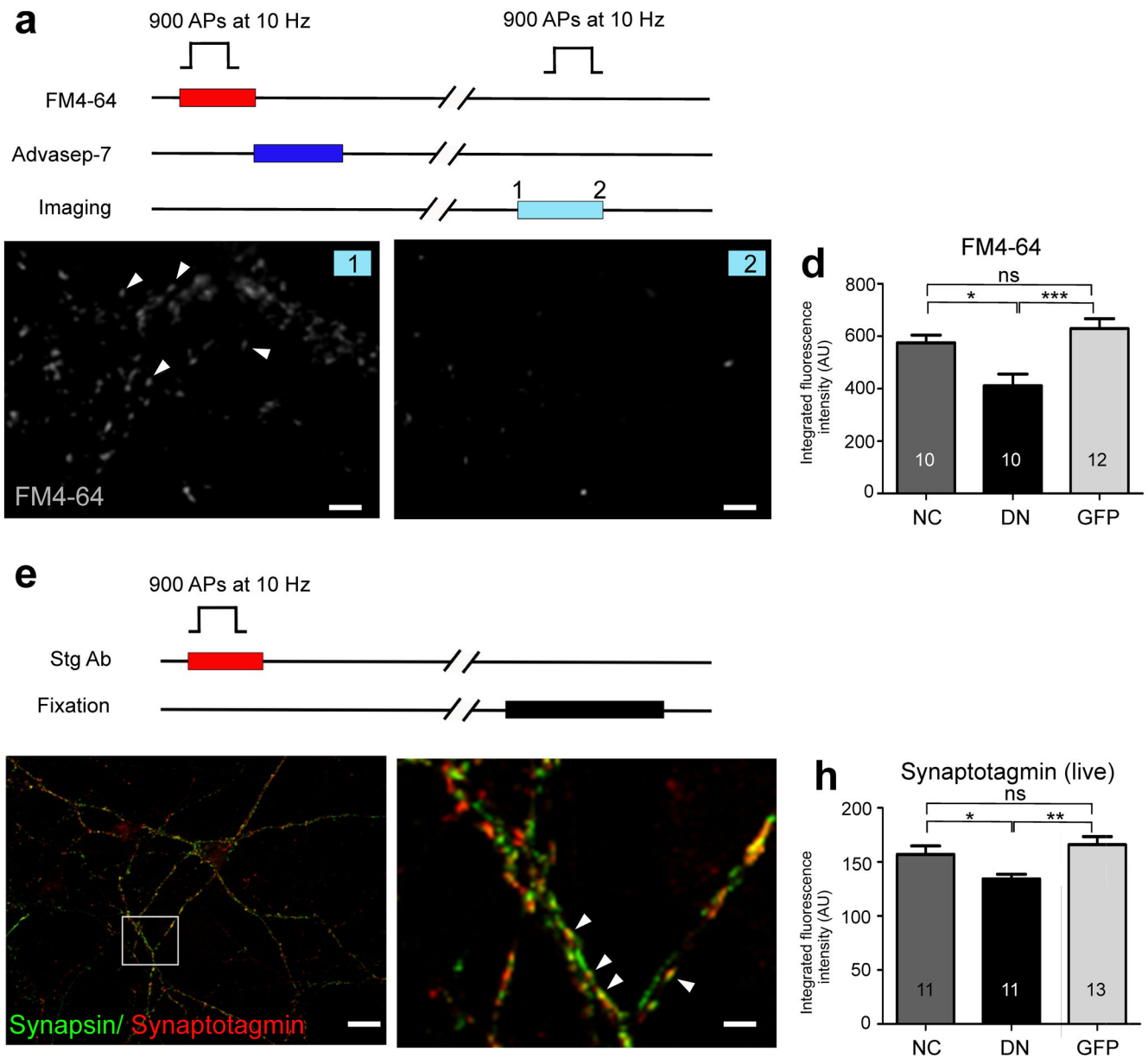

Figure 3. Disrupting postsynaptic N-cadherin activity decreases the size of the recycling SV pool

a, Scheme for FM dye experiments. **b, c,** Example images of FM4-64 dye-loaded synapses before (b) and after (c) unloading stimulation. Scale bar, 4 μm. **d,** Summary of FM4-64 fluorescence intensity of the labeled recycling vesicle pool at single synapses formed onto WT-NCad (NC), DN-NCad (DN) or GFP expressing dendrites. **e,** Synaptotagmin live labeling protocol for visualizing the recycling vesicles. **f,** Representative fluorescence image of hippocampal cultures double labeled with synaptotagmin (live) and synapsin (following fixation). Scale bar, 15 μm. **g,** Higher magnification view of the boxed region shown in f. Arrowheads indicate active boutons where two presynaptic proteins colocalize. Scale bar, 2 μm. **h,** Summary of synaptotagmin immunofluorescence intensity representing recycling vesicles at boutons formed onto NC, DN or GFP expressing dendrites. Bars show mean ± SEM. The number of neurons used is shown in bars; *P<0.05, **P<0.01, ***P<0.001, ns, no statistically significant difference; one way ANOVA followed by Tukey's test.

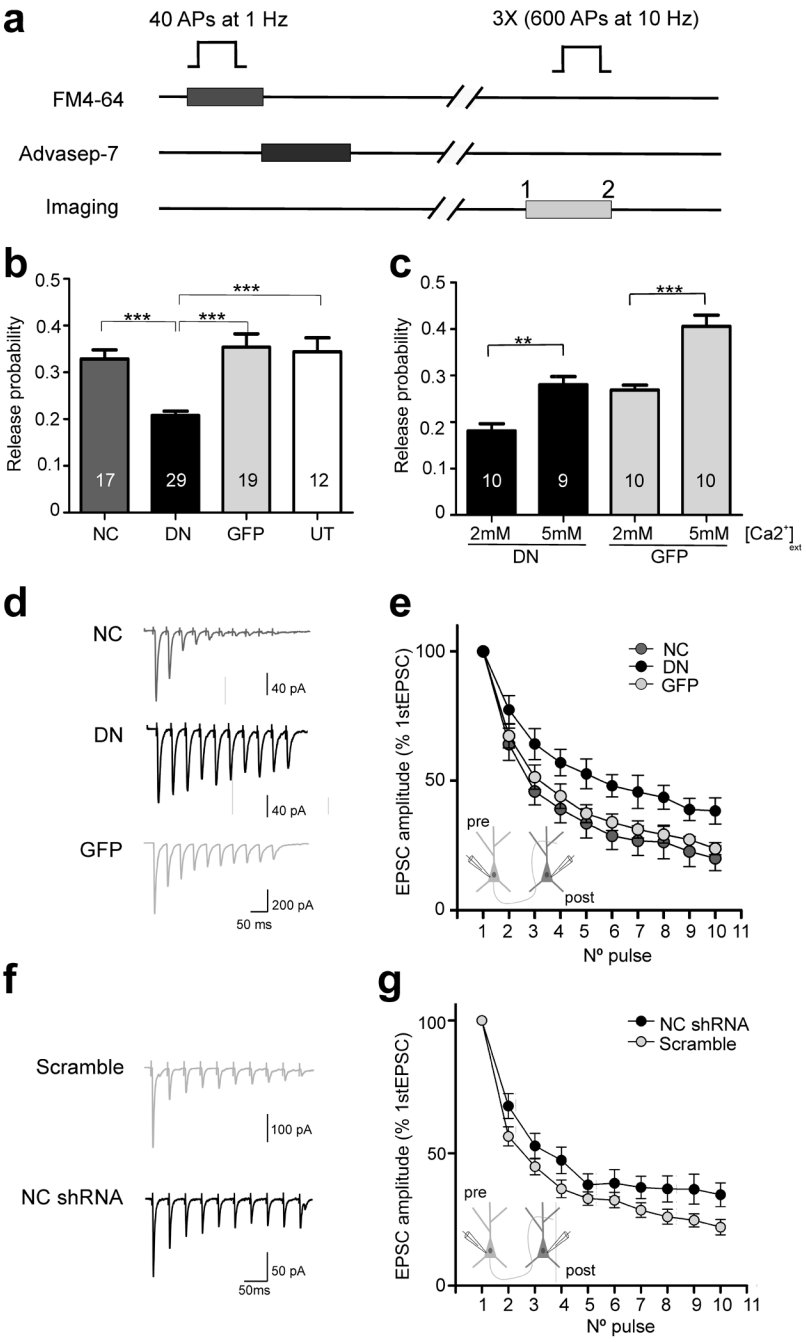

Figure 4. Postsynaptic N-cadherin modulates neurotransmitter release probability

a, Experimental protocol for estimating p_r using the optical quantal analysis. **b,** Summary of p_r at single boutons expressing WT-NCad (NC), DN-NCad (DN) or GFP postsynaptically. Untransfected cells (UT) were used as controls. **c,** Effect of increasing extracellular [Ca^{2+}] on p_r. Bars show mean ± SEM. The number of neurons used is shown in bars; **P<0.01, ***P<0.001; one way ANOVA followed by Tukey's test (b, c). **d, f,** Representative traces of EPSCs elicited by a train of 10 APs at 25 Hz from connected cell pairs in which the postsynaptic neuron overexpressed NC, DN, GFP, NC shRNA or control scramble shRNA. **e, g,** Graphs showing averaged EPSC amplitudes recorded in monosynaptically connected

postsynaptic neurons. Note the smaller depression of EPSC amplitudes for neurons overexpressing the DN compared to NC or GFP neurons (Two tailed student's *t*-test, $p<0.05$; n=11, 7, and 10 cell pairs, for NC, DN, and GFP, respectively) and the NC shRNA compared to control scramble neurons (Two tailed student's *t*-test, $p<0.05$; n=13 and 15 cell pairs for NC shRNA and scramble, respectively).

Europe PMC Funders Author Manuscripts

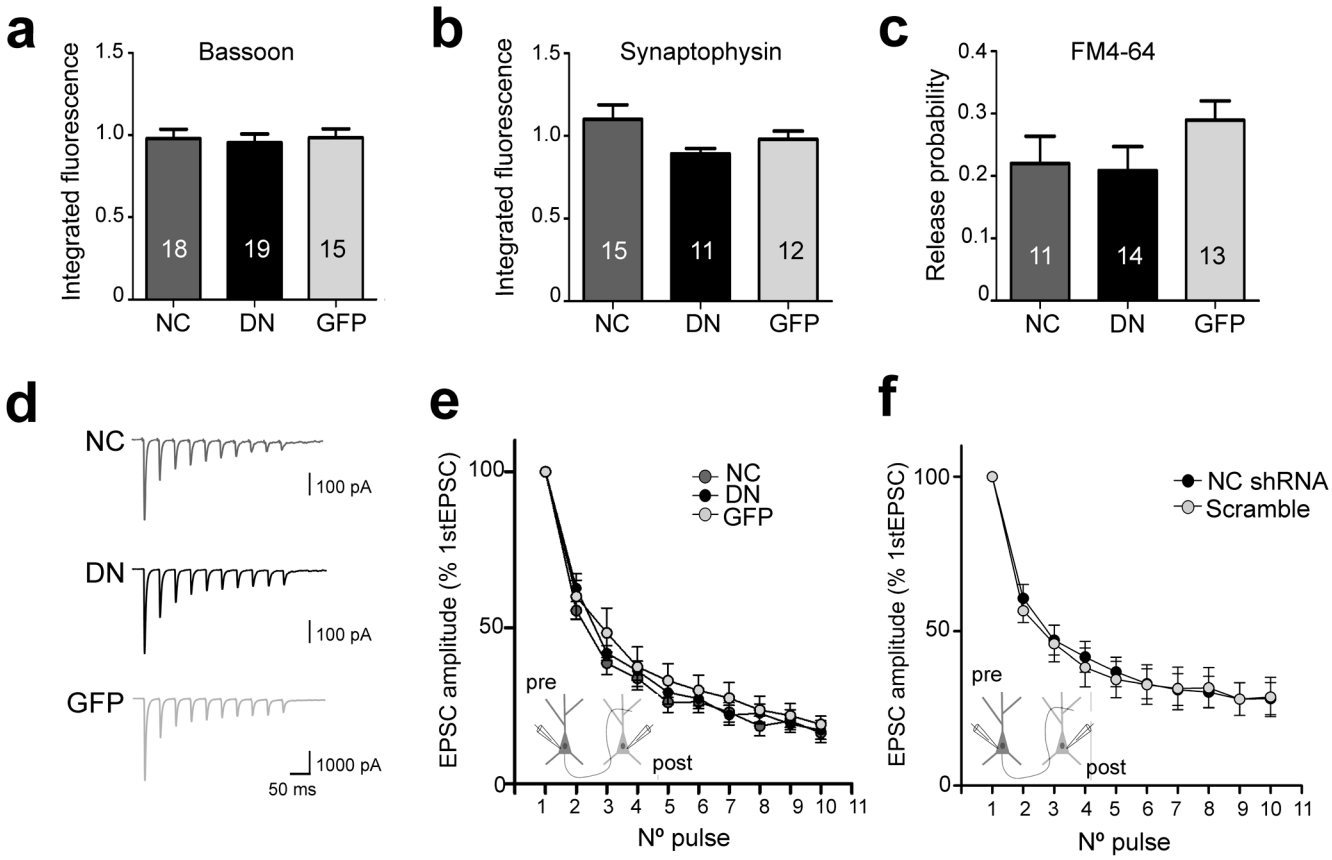

Figure 5. Presynaptic disruption of N-cadherin activity does not affect neurotransmitter release

a, b, Summary of bassoon (a) and synaptophysin (b) puncta intensity along axons expressing WT-NCad (NC), DN-NCad (DN) or GFP. Cells were double labeled for neurofilament H (with bassoon) or Tau (synaptophysin). **c,** Summary of p_r at single boutons expressing NC, DN or GFP presynaptically. The number of neurons is shown in bars. Data are mean ± SEM; one way ANOVA followed by Tukey's test; p>0.1. **d,** Representative traces of EPSC recordings elicited by a 10-AP, 25 Hz pulse train from connected cell pairs in which the presynaptic neuron overexpressed NC, DN or control GFP. **e, f,** Graphs showing averaged EPSC amplitudes recorded in monosynaptically connected cell pairs in which presynaptic neurons expressed NC (n=11), DN (n=7) or GFP (n=10) (e) and NC shRNA (n=13) or scramble (n=15) (f); two tailed student's *t*-test, p>0.05.

Europe PMC Funders Author Manuscripts

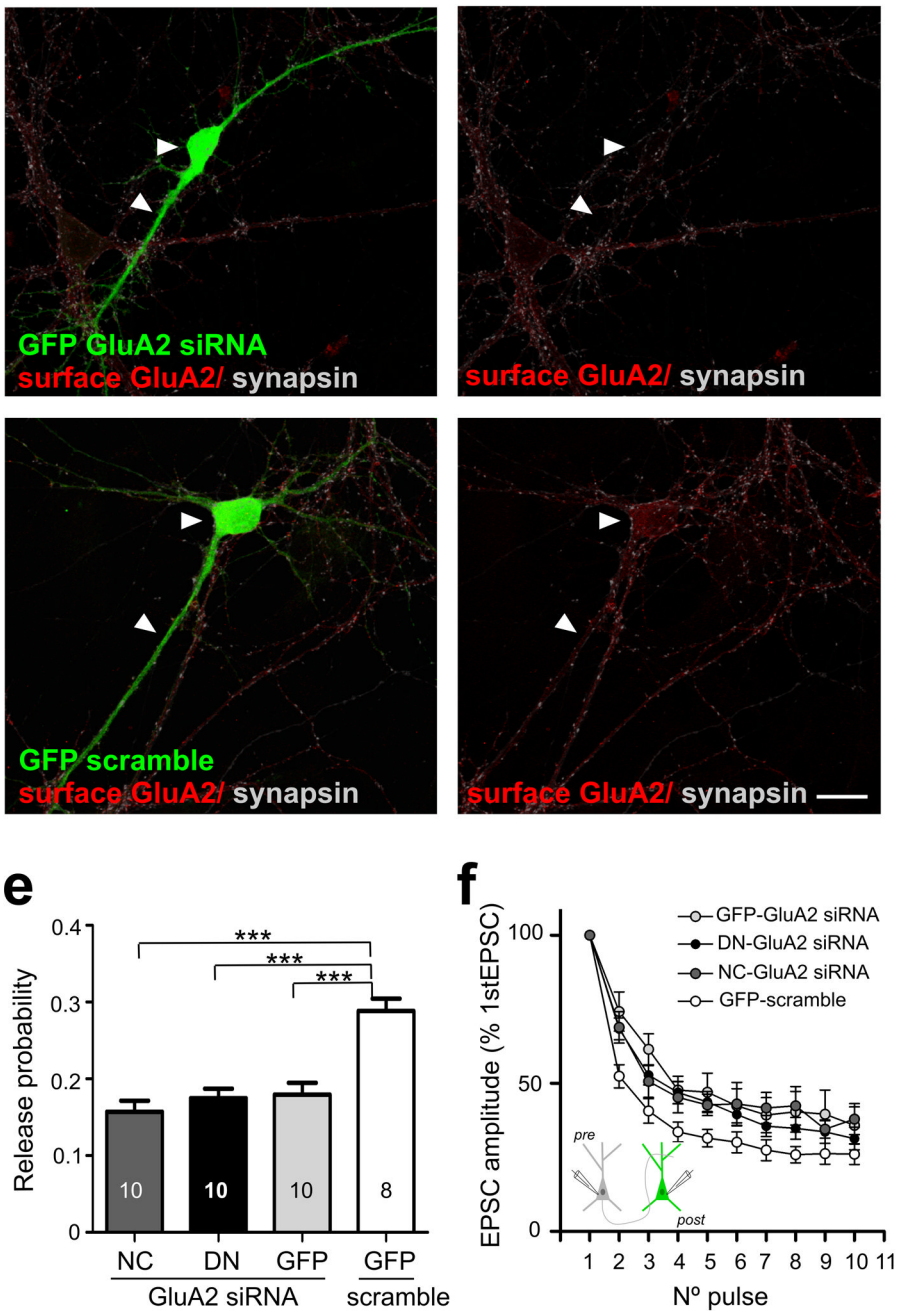

Figure 6. GluA2 is a possible effector of the transsynaptic regulation of release by N-cadherin

a, b, Hippocampal cultures expressing GluA2 siRNA show reduced levels of surface GluA2 compared to cells expressing control scrambled siRNA. **c**, Summary of p_r at single boutons co-expressing WT-NCad (NC), DN-NCad (DN) or GFP and GluA2 siRNA, or GFP and scramble control. Bars show mean ± SEM. The number of neurons used is shown in bars. ***P<0.001; one way ANOVA followed by Tukey's test. **d**, Graph showing averaged EPSC amplitudes recorded in monosynaptically connected postsynaptic neurons. Note the smaller depression of EPSC amplitudes for neurons co-expressing NC (n=7), DN (n=11) or GFP

(n=9) and the GluA2 siRNA compared to control cells co-expressing GFP and scramble (n=12). Two tailed student's *t*-test, $p<0.05$. Scale bar= 20 μm.

Europe PMC Funders Author Manuscripts

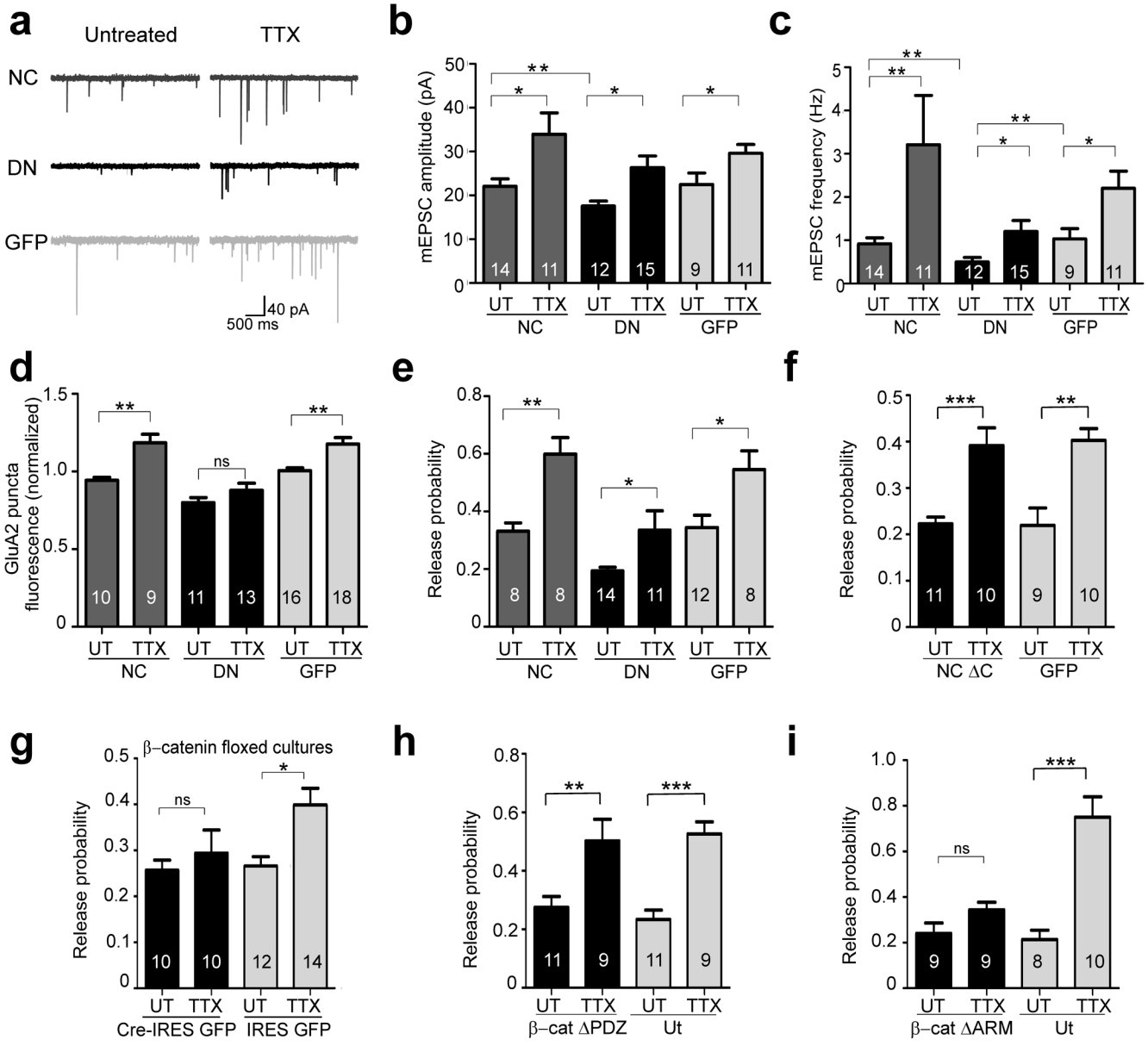

Figure 7. N-cadherin and β-catenin are differentially required for homeostatic regulation of release probability

a-c, Effects of chronically blocking network activity with TTX on mEPSC recordings from neurons expressing WT-NCad (NC), DN-NCad (DN) or GFP. Representative traces of mEPSC recordings for each condition (a). Summary of mean mEPSC amplitude (b) and frequency (c), comparing non-treated (UT) and TTX-treated groups for NC, DN or GFP neurons. Two tailed student *t*-test or Mann-Whitney test when criteria for normality were not met, P*<0.05, **P<0.01. **d,** Summary of homeostatic scaling of postsynaptic GluA2. The plot shows integrated fluorescence intensity of surface synaptic GluA2 puncta apposed to synapsin labeling in cells postsynaptically expressing NC, DN or GFP. Data are expressed as mean ± SEM relative to control untransfected neurons that are not treated with TTX. **e-i,** Effects of chronic activity block on homeostatic increase in release probability as determined by optical quantal analysis in wild type cultures on cells expressing NC, DN or GFP (e), NC ΔC or GFP (f), and β-cat ΔPDZ (h) or β-cat ΔARM (i) compared to

neighboring untransfected cells, and in β-catenin floxed hippocampal neurons transfected with Cre-IRES GFP or control IRES GFP (g). Bars show mean ± SEM. *P<0.05, **P<0.01, ***P<0.001, ns, denotes no statistically significant difference; one way ANOVA followed by Tukey's test. The number of neurons used for each group is shown in bars.

Europe PMC Funders Author Manuscripts

Europe PMC Funders Author Manuscripts

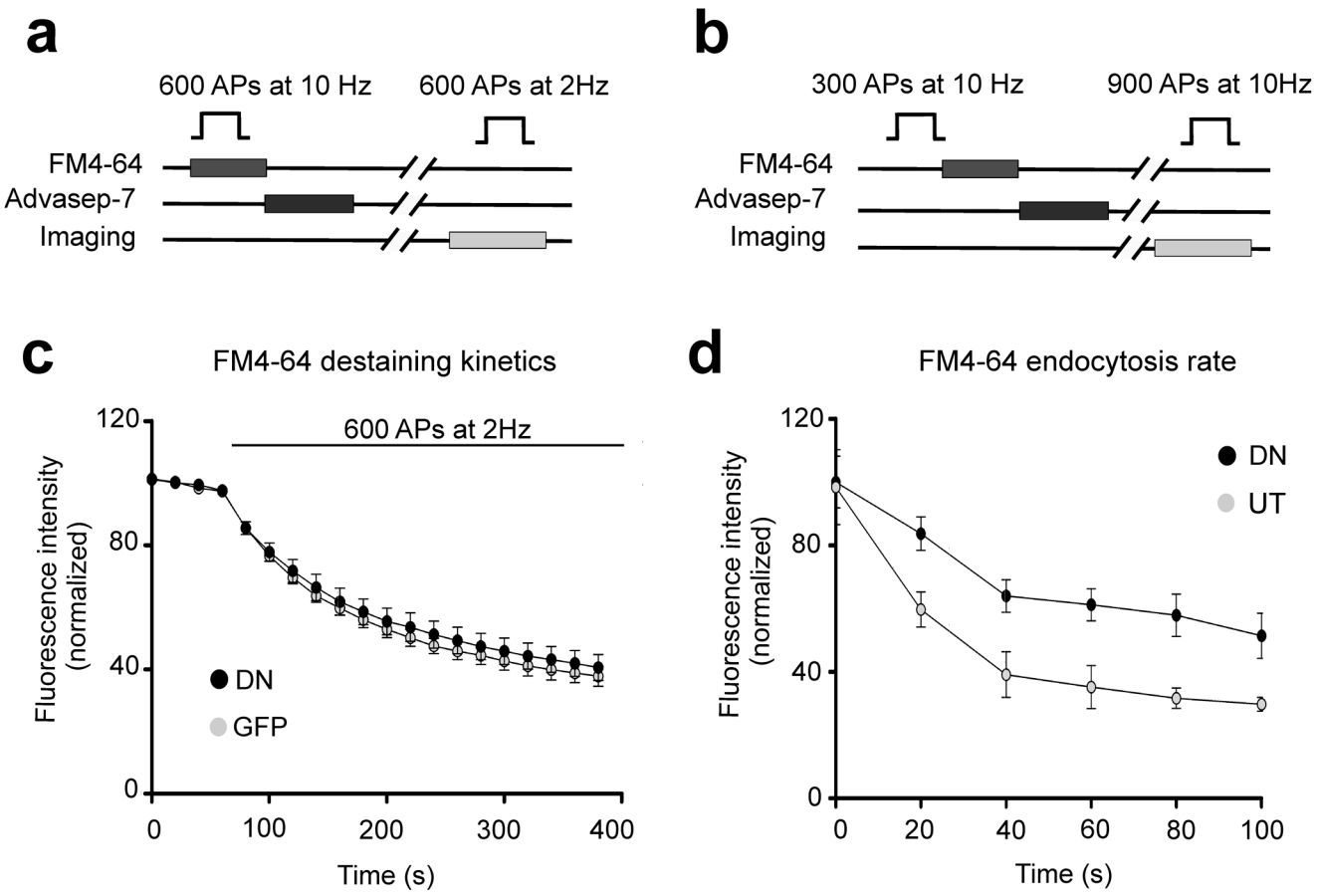

Figure 8. Disrupting postsynaptic N-cadherin activity affects SV endocytosis

a, b, Experimental scheme to analyze the kinetics of exocytosis (a) and endocytosis (b). The time course of endocytosis is measured by applying the FM dye at a variable time interval (Δt) after the end of stimulation to assess the extent of dye taken up at each time interval. **c,** Release kinetics as measured by the time course of FM4-64 destaining during 2 Hz stimulation of 600 APs [n=107 boutons for control GFP, n=140 for DN-Ncad (DN)]. **d,** Time course of endocytosis at boutons on dendrites of neurons expressing DN or on those of neighboring untransfected neurons in the same field of view. Each data point was averaged from measurements of individual boutons (DN, n=1085; UT, n= 1187) from 4-14 cells in 3 experiments.